Article

Cell Reports

Genome-wide Analysis of Host-*Plasmodium yoelii* Interactions Reveals Regulators of the Type I Interferon Response

Graphical Abstract

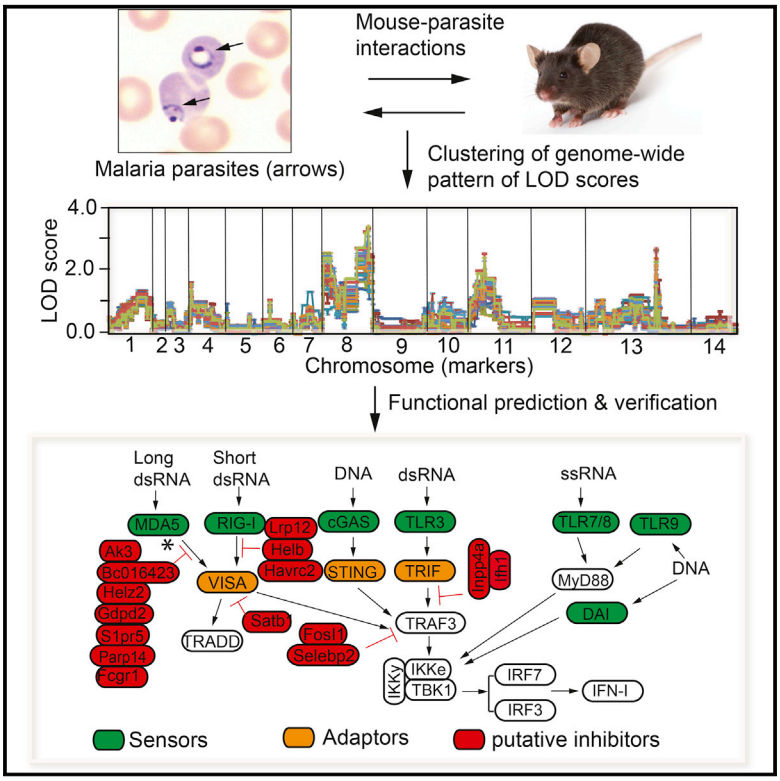

Highlights

- Trans-species eQTL links host gene expression to genetic loci of the malaria parasite
- Genome-wide pattern of LOD score clusters together genes with similar functions
- Databases of host gene clusters and linked parasite genetic loci are established
- Predicted regulators of IFN-I responses are experimentally confirmed

Authors

Jian Wu, Baowei Cai, Wenxiang Sun, ..., Timothy G. Myers, Rong-Fu Wang, Xin-zhuan Su

Correspondence

rwang3@houstonmethodist.org (R.-F.W.), xsu@niaid.nih.gov (X.-z.S.)

In Brief

Wu et al. develop an approach to study pathogen-host genetic interactions by performing trans-species expression quantitative trait locus analysis. They use patterns of genome-wide LOD scores to cluster and predict gene functions. They verify their predictions by experimental confirmation of selected genes functioning in the type I interferon pathway.

Accession Numbers

GSE63611

Wu et al., 2015, Cell Reports *12*, 661–672
July 28, 2015
http://dx.doi.org/10.1016/j.celrep.2015.06.058

Cell Reports
Article

Genome-wide Analysis of Host-*Plasmodium yoelii* Interactions Reveals Regulators of the Type I Interferon Response

Jian Wu,[1] Baowei Cai,[2,3] Wenxiang Sun,[4] Ruili Huang,[5] Xueqiao Liu,[6] Meng Lin,[3] Sittiporn Pattaradilokrat,[1,7] Scott Martin,[5] Yanwei Qi,[1,2] Sethu C. Nair,[1] Silvia Bolland,[4] Jeffrey I. Cohen,[6] Christopher P. Austin,[5] Carole A. Long,[1] Timothy G. Myers,[8] Rong-Fu Wang,[3,*] and Xin-zhuan Su[1,2,*]

[1]Laboratory of Malaria and Vector Research, National Institute of Allergy and Infectious Diseases, National Institutes of Health, Bethesda, MD 20892-8132, USA
[2]State Key Laboratory of Cellular Stress Biology, Innovation Center for Cell Signaling Network, School of Life Sciences, Xiamen University, Xiamen, Fujian 361005, PRC
[3]Center for Inflammation and Epigenetics, Houston Methodist Research Institute, Houston, TX 77030, USA
[4]Laboratory of Immunogenetics, National Institute of Allergy and Infectious Diseases, National Institutes of Health, Bethesda, MD 20892-8132, USA
[5]National Center for Advancing Translational Sciences, National Institutes of Health, Bethesda, MD 20892-8132, USA
[6]Laboratory of Infectious Diseases, National Institute of Allergy and Infectious Diseases, National Institutes of Health, Bethesda, MD 20892-8132, USA
[7]Department of Biology, Faculty of Science, Chulalongkorn University, Bangkok 10330, Thailand
[8]Genomic Technologies Section, Research Technologies Branch, National Institute of Allergy and Infectious Diseases, National Institutes of Health, Bethesda, MD 20892-8132, USA
*Correspondence: rwang3@houstonmethodist.org (R.-F.W.), xsu@niaid.nih.gov (X.-z.S.)
http://dx.doi.org/10.1016/j.celrep.2015.06.058

SUMMARY

Invading pathogens trigger specific host responses, an understanding of which might identify genes that function in pathogen recognition and elimination. In this study, we performed trans-species expression quantitative trait locus (ts-eQTL) analysis using genotypes of the *Plasmodium yoelii* malaria parasite and phenotypes of mouse gene expression. We significantly linked 1,054 host genes to parasite genetic loci (LOD score $\geq$ 3.0). Using LOD score patterns, which produced results that differed from direct expression-level clustering, we grouped host genes that function in related pathways, allowing functional prediction of unknown genes. As a proof of principle, 14 of 15 randomly selected genes predicted to function in type I interferon (IFN-I) responses were experimentally validated using overexpression, small hairpin RNA knockdown, viral infection, and/or infection of knockout mice. This study demonstrates an effective strategy for studying gene function, establishes a functional gene database, and identifies regulators in IFN-I pathways.

INTRODUCTION

After infection with a pathogen, the host mounts a coordinated response with up- and downregulation of genes functioning in various pathways (Barber, 2011). The magnitude or signature of the responses, however, depends on the specific genetic backgrounds of the invading pathogen and the host, which can be analyzed to explore gene function and gene-gene interaction and used for disease diagnosis (Mogensen, 2009). Although a large number of host receptors that recognize pathogen-associated molecular patterns (PAMPs) and immune regulators in response to infections of bacteria, viruses, and fungi have been reported (Mogensen, 2009), our understanding of the molecular mechanisms in infection responses to more complex eukaryotic organisms such as malaria parasites is still limited (Gazzinelli et al., 2014; Liehl and Mota, 2012).

Following infection, an initially strong inflammatory response has to be modulated to a balanced level to minimize damage to the host while still clearing the pathogen, and this requires activation of many immune regulators after pathogen sensing and signaling (Linkermann et al., 2014; Sakaguchi et al., 2008). For example, an early increase (24 hr) in type I interferon (IFN-I) has been shown to be associated with control of some rodent malaria infections (Liehl et al., 2014; Miller et al., 2014; Wu et al., 2014), but the level of IFN-I declines quickly (Wu et al., 2014), suggesting activation of negative regulators of IFN-I. Various IFN-I regulators have been identified (Pan et al., 2014; Peng et al., 2014), but many more are likely unknown, particularly those that are activated during infections involving complex eukaryotic organisms.

Expression quantitative trait locus (eQTL) analysis has been employed to study various phenotypes linked to gene expression (Li et al., 2012; Reilly Ayala et al., 2010), including host determinants of infection susceptibility, using progeny (Bottomly et al., 2012) or related mouse strains (Boivin et al., 2012).

Recently, several studies have reported response eQTLs (reQTL) after treating cell lines with agents such as DNase I, lipopolysaccharide (LPS), interferon-β (IFN-β) or IFN-γ, influenza virus, or *Mycobacterium tuberculosis* (MTB) (Barreiro et al., 2012; Degner et al., 2012; Fairfax et al., 2014; Lee et al., 2014). These studies have identified candidate genes playing important roles in response to various stimulations; however, they generally map eQTLs within the same species, i.e., using progeny of host genetic crosses, closely related strains, or cell lines in vitro after stimulation with a microorganism or chemical or biological agents. Stimulation of host responses through infection with pathogens of related but distinct genetic backgrounds might have the advantage of recapitulating complex host-pathogen interactions, which is one of the goals of this study.

Here, we employ a unique strategy termed trans-species eQTL (ts-eQTL) to identify parasite genetic loci linked to host gene responses and predict host gene functions (Figure 1A). We treated the expression levels of ~20,000 host genes as phenotypes after infection with progeny from a genetic cross of two variants of the rodent malaria parasite *Plasmodium yoelii* (Li et al., 2011) and found that many host gene responses to the parasite infections were "inheritable," leading to significant linkages of a large number of host genes and parasite genetic loci. Importantly, we found that clustering of genome-wide patterns of LOD scores (GPLSs) allowed accurate functional prediction of unknown host genes. This study establishes a database of gene clusters for further functional characterizations and identifies many previously unknown regulators of type I interferon (IFN-I) responses. Additionally, a large number of parasite genetic loci/chromosome segments linked to host gene responses were also identified.

RESULTS

Inheritable Host Gene Expression in Response to Malaria Infection

We infected C57BL/6 (N strain) mice with two haploid malaria parasites (*P. yoelii yoelii* 17XNL and *P. yoelii nigeriensis* N67) having dramatically different disease phenotypes and 24 progeny of a genetic cross between them (Li et al., 2011). We extracted mRNA from mouse spleens (three mice for each parasite) 4 days postinfection (p.i.) and hybridized the mRNA samples to the Illumina Mouse-Ref8 v2, targeting ~25,600 annotated RefSeq transcripts and >19,100 unique genes. After processing signals from array hybridizations, we obtained 9,701 genes (12,951 probes) that had significant differences (false discovery rate [FDR] < 0.05) in mRNA levels between the infected and the naive mice and 1,089 genes between the mice infected with the two parents (Table S1), including 112 genes (137 probes) with ≥2-fold differences (Table S2). Clustering analysis showed diverse gene expression patterns in mice infected with different individual progeny and many of the progeny in clusters separated from the parents (Figure S1A). These results suggest generation of new expressional phenotypes. However, the progeny were clearly clustered into two groups, each associated with one of the parents if we used the 112 highly differentially expressed genes, with clusters containing upregulated genes mostly encoding cytokines/chemokines or downregulated genes related to hematopoiesis or blood cell development (Figure S1B; Table S2). Closer examination of the expression data revealed "inheritance" of high or low host gene expression levels in the mice infected with different parasite progeny (Table S2), suggesting that the expression levels of host genes in response to infections with different parasite progeny were directly influenced by specific parasite genes and can be studied as Mendelian traits.

Hyper-Interactive Parasite Chromosomes

To investigate the effects of parasite genes on host gene expression, we performed genome-wide ts-eQTL analysis of differentially expressed host genes against 479 microsatellite (MS) markers typed on the parasite progeny (Li et al., 2011) and significantly (LOD score ≥ 3.0) linked 1,054 host genes to 208 unique parasite MS markers/loci, identifying 6,957 significant host gene-parasite marker interactions (Figure 1B; Tables S3 and S4). Among the 1,054 genes, at least 80 were annotated as mRNA or cDNA transcripts without any functional prediction. Interestingly, plotting the numbers of host genes significantly (LOD score ≥ 3.0) linked to each marker across the parasite chromosomes showed dramatic differences in the distribution of host genes linked to markers across the 14 parasite chromosomes, with chromosomes 3, 4, 8, 9, 10, 13, and part of 14 having markers (or parasite genes) linked to more host genes, particularly chromosomes 8, 10, and 13, than the other chromosomes (Figure 1C). These results suggest that some parasite chromosomes are more "interactive" (or i-chromosomes) than others. Additionally, significantly ($p < 1E-20$) more markers at subtelomeric regions (defined as 150 kb from chromosome ends) than at "central" regions of the same sizes were linked to host genes with LOD scores ≥ 3.0, which is consistent with the presence of many antigenic gene families at the subtelomeres (Carlton et al., 2002). A plot of parasite markers significantly linked to host genes also showed some host genes interacting with more markers than others, although many of the markers were physically linked and should be treated as one locus due to the lack of genetic recombination between the markers (Figure 1D). If we reduced the cutoff LOD score to ≥ 2.0 (suggestive linkage), we detected 72,549 interactions involving 6,417 host genes in 644 clusters (Table S5). Plots of the numbers of host genes linked to the parasite markers showed patterns parallel to those obtained from the gene list of LOD ≥ 3.0 (Figures 1C and 1D). These results clearly show complex interactions involving large numbers of genes from both malaria parasites and their rodent hosts.

Networks of Host-Parasite Gene Interaction and Functional Enrichment

To further investigate the relationships of host gene-parasite marker interactions, we constructed a network of host gene-parasite marker interactions by connecting each linkage with LOD score ≥ 3.0 using Cytoscape V3.0 (Shannon et al., 2003) and showed clusters of host genes interacting with various parasite markers (Figure 2A). Gene Ontology (GO) term enrichment analysis of the host genes significantly linked to parasite markers revealed significant associations of a parasite marker (or markers) with host genes in specific functional GO terms (Table S6). For example, marker Py345 on chromosome 4 was

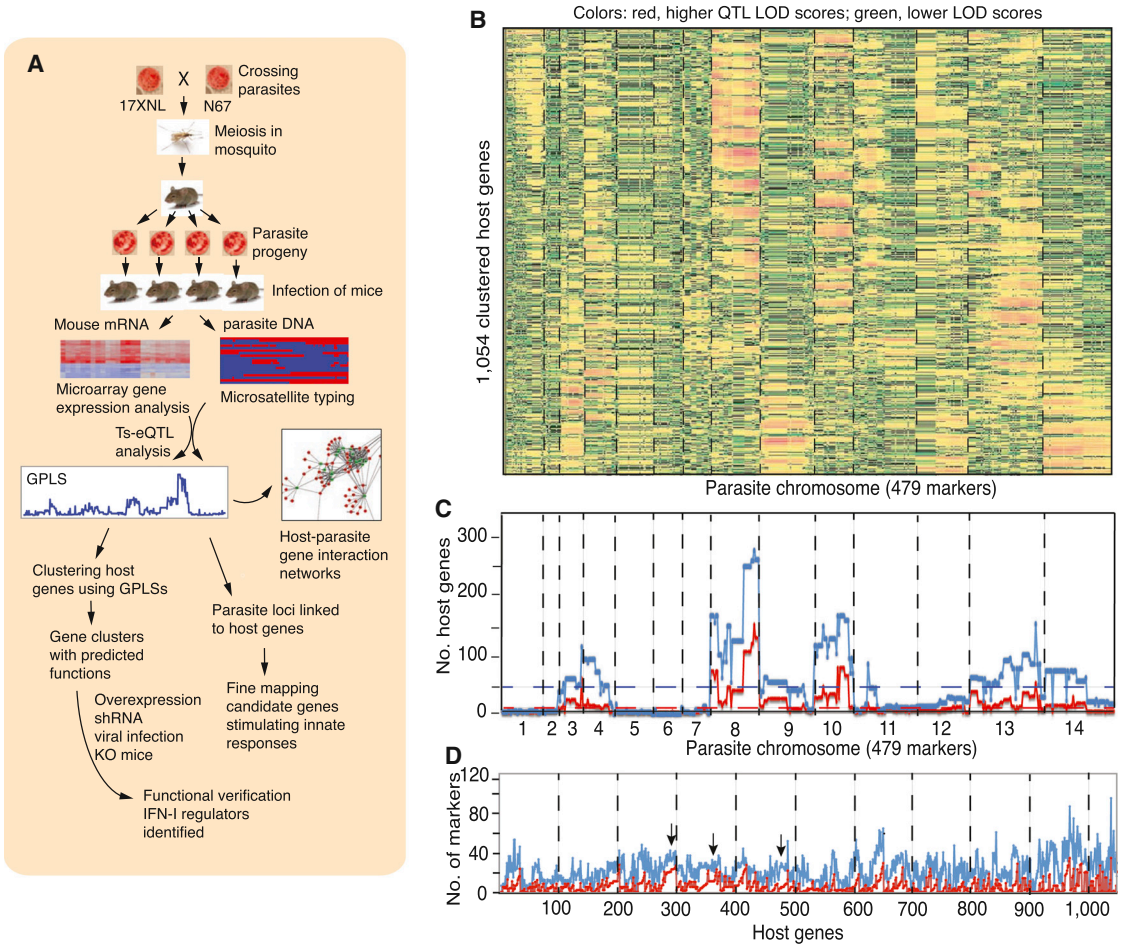

Figure 1. Genome-wide Gene Interactions of Malaria Parasites and Their Hosts

(A) Diagram showing strategies to identify genome-wide gene interactions between the *Plasmodium yoelii* parasite and C57BL/6 mice, predict host gene function, and verify regulators of host innate responses.

(B) Heatmap of genome-wide LOD scores of host genes significantly (LOD scores $\geq$ 3.0) linked to at least one parasite microsatellite (MS) marker. Host genes are clustered by similarity of their genome-wide pattern of LOD scores (GPLSs). Red color indicates higher LOD scores, whereas green indicates lower LOD scores (see Table S3 for gene list).

(C) Plots of numbers of host genes linked to each MS marker on the parasite's 14 chromosomes with cutoff LOD scores $\geq$ 3.0 (red line) or $\geq$ 2.0 (blue line), respectively. The red dashed line indicates mean number of genes (14.5) linked to a marker at LOD score $\geq$ 3.0; the blue dashed line indicates the mean number of genes (50.9) at LOD score $\geq$ 2.0.

(D) Plots of numbers of MS markers linked to host genes that were linked to at least one marker at an LOD score $\geq$3.0.

significantly linked to 52 host genes enriched for response to ATP (GO:0033198, FDR = 4.6E-17), adenine phosphoribosyltransferase activity (GO:002999, FDR = 7.7E-12), and positive regulation of IL-1β secretion (GO:0050718, FDR = 2.2E-6) (Figure 2B; Table S6). A host gene could also be linked to more than one parasite marker, although the markers were often at the same physical locations. The results suggest that functional relationships of host and parasite genes govern the patterns of host gene-parasite marker interaction networks.

Genes with Similar GPLSs Functioning in Related Pathways

Consistent with the interaction patterns and GO-term enrichment, plotting and comparison of GPLSs across the 14 parasite chromosomes for individual genes revealed similar GPLSs for host genes functioning in the same or related biological pathways. For example, several genes in IFN-I response pathways, from the regulator of *Ifih1/Mda5* (*Dhx58 or Lgp2*) to transcription factors (*Irf7* and *Stat2*) to IFN-I induced protein (*Oas1g*), had similar GPLSs with a major peak on chromosome 13 and some minor peaks on chromosomes 4, 10, and 12 (Figures 3A–3D). To further test the hypothesis that genes functioning in the same pathway have similar GPLSs, we clustered the 1,054 linked genes with LOD score $\geq$ 3.0 and the 6,417 genes with LOD score $\geq$ 2.0 into 348 and 644 groups, respectively, based on the similarity of their GPLSs using the self-organizing map (SOM) algorithm (Kohonen, 2006) (Tables S3 and S5). GO-term enrichment analysis of genes in each cluster showed significant

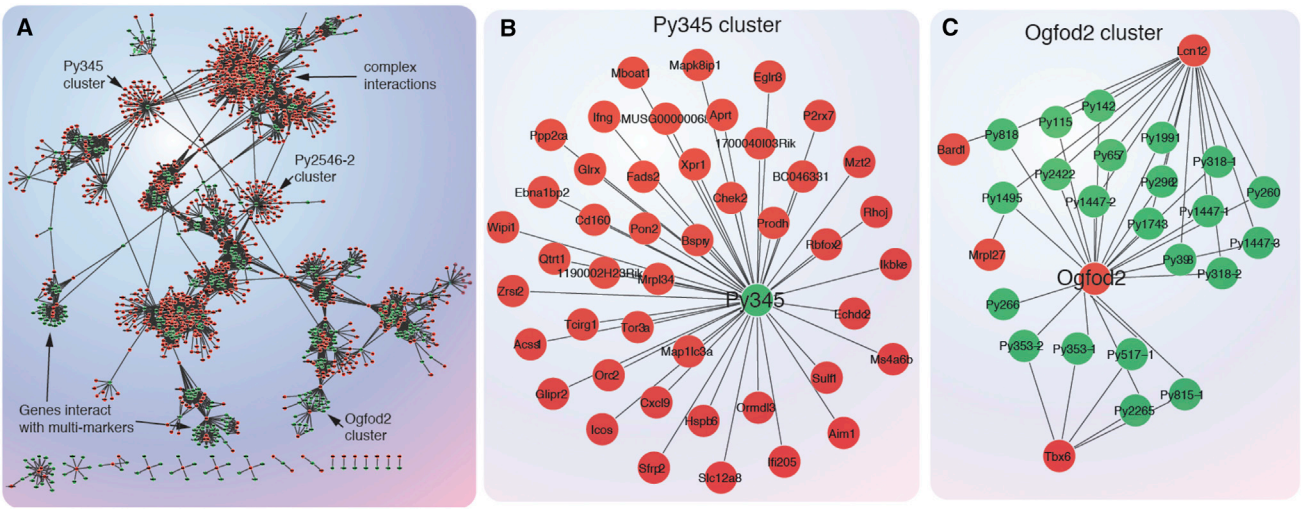

Figure 2. Networks of Significant Interactions between Parasite Markers and Host Genes

(A) A genome-wide host gene-parasite marker interaction network connected by lines with a linkage of LOD score ≥ 3.0. Each red dot represents a host gene, and each green dot represents a parasite marker.

(B) A cluster of host genes, enriched in GO terms of response to ATP, adenine phosphoribosyltransferase activity, and positive regulation of IL-1β secretion, interacting with parasite marker Py345 on chromosome 4.

(C) Five host genes interacting with multiple parasite markers that are on the same locus of parasite chromosome 14. The network image is zoomable on the monitor.

enrichment of genes in specific pathways. For example, cluster 71 was significantly enriched for genes in water transport and glutathione peroxidase activity (FDR = 1 × 1.00E-17), and cluster 220 was enriched with genes functioning in double-stranded RNA adenosine deaminase activity (FDR = 1 × 1.07E-11) and 2′-5′-oligoadenylate synthetase activity (FDR = 4.60E-8) (Table S7). These results suggest that each cluster likely contains functionally related genes.

To further investigate the functionality of the clusters, we searched the 644 clusters for selected known genes functioning in the IFN-I pathways and found that many of the known IFN-I induced genes were in clusters 219, 220, 243, or the nearby clusters (Tables S5 and S8). Plots of GPLSs from the 32 genes in cluster 219, 220, and 243 showed very similar patterns, all having a major peak at one end of chromosome 13, a secondary peak on chromosome 10, and a third peak on chromosome 4 (Figure 3A-3E). Among the 32 genes in the three clusters, at least 16 (50%; *Oas1g*, *Tgfb3*, *Tnfrsf12a*, *Stat2*, *Parp14*, *Oas1a*, *Adar1*, *Mx2*, *Irf7*, *S1pr5*, *Oas2*, *Dhx58*, *Ifit3*, *Usp18*, *Isg15*, and *Ifi35*) were known to play a role (or induced by) in the IFN-I response (Chapman et al., 2013; Eskan et al., 2008; George et al., 2011). Search of an interferon database (Rusinova et al., 2013) identified an additional nine genes (*Hbegf*, *Cstb*, *Fcγr1*, *Tnc*, *Errfi1*, *Wisp1*, *Kazad1*, *Rtp4*, and *B430306N03Rik*) that have been implicated in the IFN-I response, increasing the percentage to 78.1% (25/32). Using Ingenuity Pathway Analysis (IPA), our analysis of the 156 genes in expanded clusters containing either one or more IFN-I related genes and/or those neighboring clusters 219, 220, and 243 (Table S8) showed that the top three canonical pathways were interferon signaling, activation of IRF by cytosolic pattern recognition, and PKR interferon induction in the antiviral response, and that one of the top interactive networks included many IFN-I-related genes (Figure 3F). These results confirm that GPLS clustering groups genes functioning in the same or related pathways, which can be explored for predicting functions of unknown genes. For example, BC006779 (or *Helz2*) and *Lrp12* in cluster 220 are not known to function in IFN-I pathways; however, because they are clustered with many known IFN-I-related genes, they are predicted to function in IFN-I response.

The growth of malaria parasites requires a continuous supply of new red blood cells (RBCs), particularly for *P. y. yoelii* 17XNL that mainly invades reticulocytes (Büngener, 1979) and strongly stimulates hematopoiesis. GO-term enrichment analysis on the 6,417 genes showed that the top enrichment groups contained GO processes of heme biosynthesis, long-chain fatty acid metabolism, one-carbon compound transport, and erythrocyte differentiation. Search for genes in porphyrin/heme metabolism (genes in GO process #GO:0006779, FDR = 2.5E-3, and #GO:0006778, FDR = 4.7-3; erythrocyte differentiation, #GO:0030218, FDR = 1.6-1) or known genes encoding selected RBC proteins such as RHAG and HBb identified 12 clusters (5, 9, 24, 26, 27, 48, 49, 50, 51, 70, 71, and 93) containing 214 genes with diverse predicted functions as well as functions in hematopoiesis, heme metabolism, or gas or solute transport (Table S9). Among these genes, nine were also significantly associated with human blood cell phenotypes according to a recent genome-wide association analysis (van der Harst et al., 2012). Amazingly, the GPLSs for 26 genes randomly selected from the 12 clusters were almost identical with four major peaks: two on chromosome 8, one on chromosome 11, and one on chromosome 13 (Figure 4A). As expected, the top IPA canonical pathways produced from the 214 genes included heme biosynthesis II (Figure 4B), tetrapyrrole biosynthesis II, and superoxide radical

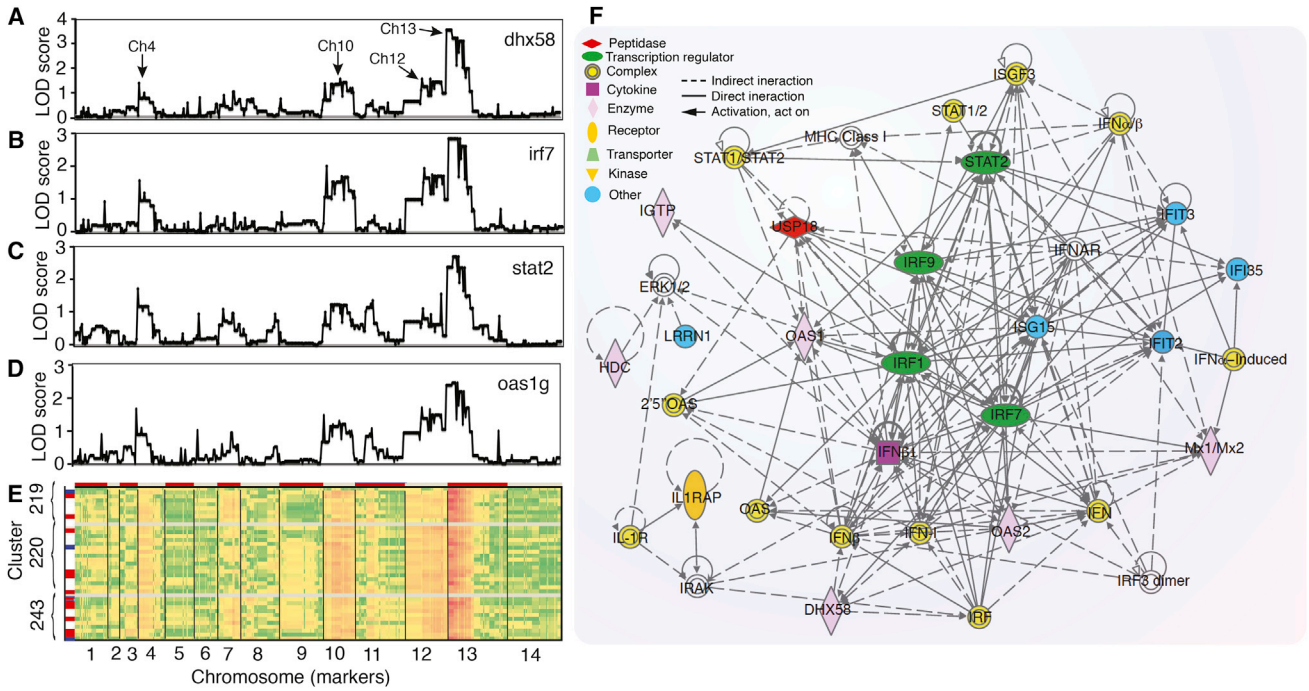

Figure 3. Similar Genome-wide Pattern of LOD Scores for Genes Functioning in Type I Interferon Pathways in Response to Infection of Progeny from the *Plasmodium yoelii nigeriensis* N67 and *Plasmodium yoelii yoelii* 17XNL Genetic Cross

(A–D) GPLSs from four genes known to play a role in IFN-I response. *Dhx58*, probable ATP-dependent RNA helicase; *Irf7*, interferon regulatory factor 7; *Stat2*, signal transducer and activator of transcription 2; and *Oas1g*, 2′-5′ oligoadenylate synthetase 1g.

(E) Heatmaps of genome-wide LOD scores of genes in clusters 219, 220, and 243 that contain many known IFN-I-related genes; red, higher LOD scores; green, lower LOD scores, as reflected in the curves above.

(F) A gene interaction network of antimicrobial and inflammatory responses constructed based on genes in the IFN-I related clusters (Table S8) using Ingenuity Pathway Analysis (IPA). Molecules without color are not present in the gene lists.

degradation; among the top gene interaction networks was hematological system development and function (Figure 4C). Interestingly, 17 genes in cluster 23 contained *Smad5* in the erythrocyte differentiation GO process (GO:0030218); however, these genes had GPLSs different from the genes in the 12 clusters with a major peak on chromosome 10 (Figure S2A). SMAD5 plays a role in the transforming growth factor β (TGF-β)-mediated pathway inhibiting the proliferation of hematopoietic progenitor cells (Larsson and Karlsson, 2005), and the tight clustering of the GPLSs for the 12 genes suggests that these genes may function in SMAD5-related pathways, negatively regulating host hematopoiesis. Other interesting clusters were cluster 640, which contained 12 histone genes that should have similar functions (Figure S2B), and cluster 277, which contained 11 genes, including the *Fas* gene and five others known to be associated with apoptosis (Figure S2C). These results again support the validity of functional clustering of genes using GPLS, which in turn can be explored for generating hypotheses on the functions of unknown genes.

Parasite Genetic Markers Significantly Linked to Host Genes

In addition to the identification of host gene clusters with predicted functions, our analyses also significantly (individual LOD score ≥ 3.0) linked 1,054 host genes to 208 unique parasite genetic markers/loci (Table S4). Among the 208 markers, 122 were unique primary markers that had the highest LOD scores (LOD1; Table S4), and 86 had the secondary highest LOD scores on chromosomes different from those of the primary markers (LOD2), suggesting that there were many host genes significantly linked to two parasite genetic loci on different chromosomes. We next examined the genotypes of the progeny to identify crossovers and identified 96 unique haplotypes or independent chromosome segments (Li et al., 2011) (Tables S3 and S5). There were also markers with LOD scores different from those of flanking markers not associated with recombination events. The changes in LOD scores for these markers were likely due to missing genotype data, and any significant linkages for these markers would need to be further confirmed after filling in the missing genotype data.

Although many linked parasite loci typically represent chromosomal segments greater than 100 kb in size, there were also loci with recombination events leading to relatively small chromosome segments. One example was the major peak on chromosome 8 (represented by marker Py20321) that was significantly linked to genes functioning in hematopoiesis or RBC surface molecules, including the gene encoding glycophorin A (Figures 4A and 4D). Examination of the MS marker inheritances among the progeny typed previously (Li et al., 2011; Pattaradilokrat et al., 2014) found two progeny (G001#4 and F117#2) having

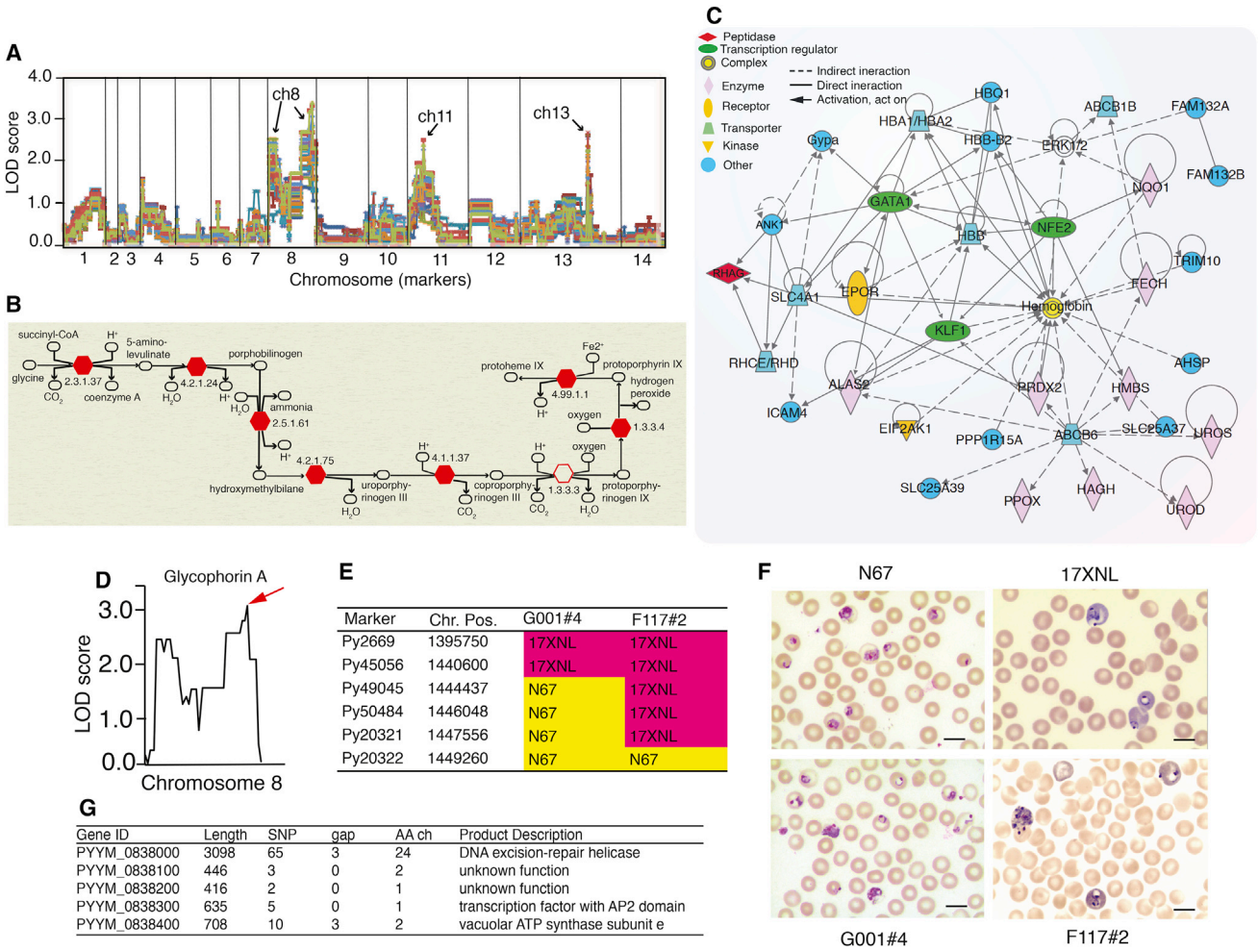

Marker	Chr. Pos.	G001#4	F117#2
Py2669	1395750	17XNL	17XNL
Py45056	1440600	17XNL	17XNL
Py49045	1444437	N67	17XNL
Py50484	1446048	N67	17XNL
Py20321	1447556	N67	17XNL
Py20322	1449260	N67	N67

G

Gene ID	Length	SNP	gap	AA ch	Product Description
PYYM_0838000	3098	65	3	24	DNA excision-repair helicase
PYYM_0838100	446	3	0	2	unknown function
PYYM_0838200	416	2	0	1	unknown function
PYYM_0838300	635	5	0	1	transcription factor with AP2 domain
PYYM_0838400	708	10	3	2	vacuolar ATP synthase subunit e

Figure 4. Genome-wide Pattern of LOD Scores and Interaction Network of Selected Genes in Hematopoiesis and Mapping a Parasite Locus Linked to Glycophorin A

(A) GPLSs of 26 genes randomly selected from the 12 clusters associated with erythrocyte differentiation and heme metabolism (Table S9). The genes are *Atpif1*, *Exoc6*, *Zfpm1*, *Alad*, *Thra*, *Dyrk3*, *Tal1*, *Ank1*, *Slc25a39*, *Ppox*, *Icam4*, *Fech*, *Urod*, *Uros*, *Darc*, *Tfdp2*, *Nfe2*, *Blvrb*, *Tmem14c*, *Rhag*, *Aqp1*, *Car2*, *Klf1*, *Gypa*, *Alas2*, and *Ahsp*.

(B) The top canonical pathway (heme biosynthesis II) constructed based on the genes in the 12 clusters using IPA. All the enzymes were present in the clusters except coproporphyrinogen oxidase (1.3.3.3).

(C) One of the top interaction networks (hematological system development and function) constructed based on genes in the 12 clusters using IPA.

(D) Plot of LOD score on chromosome 8 showing a major peak significantly linked to host glycophorin A (arrow).

(E) Genetic marker positions and crossovers in the chromosome 8 locus in progeny G001#4 and F117#2. Yellow color under progeny name indicates N67 genotype and phenotype; red indicates 17XNL genotype and phenotype (higher expression and invading reticulocytes only). Primer sequences for the new MS markers: Py45056, 5′-AAAAAGCGTAATGAATTGTC-3′ and 5′–ATTTTTACCAAACCTACTTG-3′; Py49045, 5′-GTATAAGGATGTACAAATG-3′ and 5′-TTCGTTAGTTTCCTTCGATT-3′; Py50484, 5′-GATGGTGTATGCATTTTTAT-3′ and 5′-ATTGTATTCATATTTTCGCG-3′.

(F) Microscopic images of blood smears showing cell types invaded by N67, 17XNL, and the two progeny. Reticulocytes are larger and stained darker than mature red blood cells. Scale bar, 10 μm.

(G) Candidate genes in the locus showing polymorphic sites between N67 and 17XNL parasites. DNA sequences from N67 were obtained from genome sequences as described previously (Nair et al., 2014), and those of 17XNL were from PlasmoDB (http://plasmodb.org/plasmo/). SNP, single-nucleotide polymorphism; gap, size polymorphism; AA ch, amino acid changes. Product descriptions are from PlasmoDB.

crossovers between MS markers Py2669 and Py20322 at the locus (~53.5 kb apart), which was responsible for the decline of LOD scores in the flanking regions (Figure 4E). The normalized log2 expression signal of glycophorin A for F117#2 was −0.44, similar to that of 17XNL (−0.08), whereas G001#4 was −3.81, more similar to that of N67 (−1.6) (Table S2). Examination of blood smears also showed that F117#2 invaded reticulocytes and stimulated hematopoiesis as 17XNL did, and both N67 and G001#4 could invade normocytes (Figure 4F). To define the locus more precisely, we identified additional MS markers within the locus to fine-map the crossover sites (Figure 4E) and reduced the locus to an ~8.7-kb DNA segment containing five

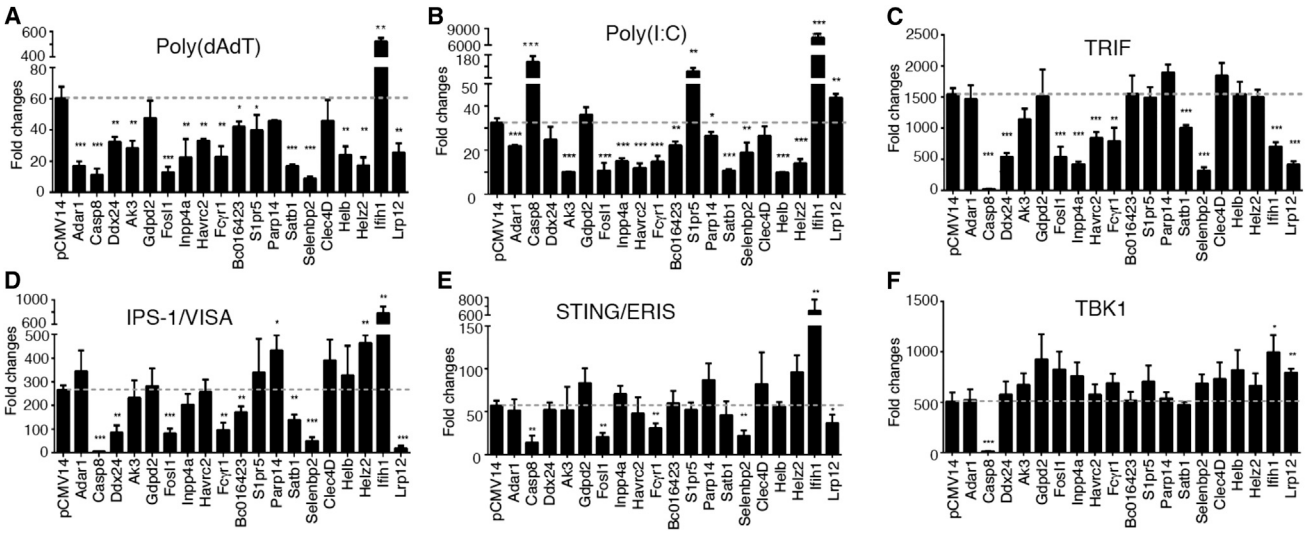

Figure 5. Changes in Luciferase Signals after Co-transfection of Plasmids Expressing Candidate Genes or Stimulation with Poly(dAdT) or Poly(I:C)

(A and B) Fold changes in luciferase signal in 293T cells expressing luciferase under the control of an IFN-I-responsive promoter after expression of indicated genes and then stimulation with poly(dAdT) or poly(I:C), respectively.

(C–F) Fold changes in luciferase signal after co-transfection of the same cell line with plasmids containing indicated gene plus gene encoding TRIF (C), MAVS (D), STING/ERIS (E), or TBK1 (F). pCMV14 is the vector control, and the horizontal dotted line is the level of activity with empty vector in addition to the stimuli shown in (A)–(F); all the genes were cloned into the pCMV14 expression vector. *$p < 0.05$; **$p < 0.01$; ***$p < 0.001$(t test; SDs from three replicates).

candidate genes, including a gene encoding a DNA excision-repair helicase that has three size polymorphisms and 24 amino acid substitutions between 17XNL and N67 (Figure 4G). Further functional characterizations of the candidate genes are necessary to determine if the gene(s) really plays a role in stimulating host hematopoiesis.

Similar to the GPLS clustering, a parasite marker or locus was often significantly linked to multiple host genes in the same functional clusters discussed above. For example, 9 of the 11 genes in cluster 277 (*Ccr5*, *Fas*, *Hmgcl*, *Qpct*, *Stat4*, *Tsen15*, *Crat*, *Gpr171*, and *E2f1*) were significantly linked to markers Py2032, Py1440, and Py1654 located at one end of chromosome 8 (Figure S2C; Tables S3 and S5). This locus represented a linkage group neighboring but different from the one linked to glycophorin A (Table S3). Similarly, many IFN-I-related genes in clusters 219, 220, and 243 (*Oas1g*, *Hbegf*, *Tgfb3*, *Tnfrsf12a*, *Fcgr1*, *Pxmp4*, *B430306N03Rik*, and *Dhx58*) were significantly linked to markers (Py712, Py1300, and Py521) at one end of chromosome 13 (Figure 3E; Table S5). The linkages of multiple genes functioning in related pathways to the same locus can be considered as equivalent to multiple repeats, which supports the interactions of the specific host and parasite genes.

Suppression of Luciferase Signals by Expression of Predicted IFN-I-Induced Genes

To experimentally verify the accuracy of GPLS in predicting gene function, we co-transfected 293T cells with plasmids containing 14 candidate genes randomly selected (4 mouse and 10 human genes) from the IFN-I related clusters, a luciferase reporter plasmid driven by the IFN-β promoter (IFN-β luciferase), and a plasmid containing Renilla luciferase as control (Table S10; Figure 5). We also included three known negative regulators of IFN-I responses (*Adar1* in cluster 220, *Casp8* in cluster 241, and *Ddx24* in cluster 18) (Ma et al., 2013; Rajput et al., 2011; Wang et al., 2008), a positive control *Ifih1* (MDA5), and pCMV14 vector as transfection controls. Stimulation of the cells with poly(dAdT) 24 hr after introduction of the plasmids containing *Ak3*, *Fosl1*, *Inpp4a*, *Havcr2*, *Fcγr1*, *Bc016423*, *S1pr5*, *Parp14*, *Satb1*, *Selenbp2*, *Helb*, *Helz2*, *Lrp12*, and the three known negative regulators showed significant reduction ($p < 0.05$, Student's t-test; same for the rest) in IFN-β-luciferase activity, whereas *Ifih1* greatly increased the luciferase signal (Figure 5A). Similarly, *Ak3*, *Fosl1*, *Inpp4a*, *Havrc2*, *Fcγr1*, *Bc016423*, *Parp14*, *Satb1*, *Helb*, and *Helz2* significantly downregulated the luciferase signal, whereas *Casp8*, *S1pr5*, *Lrp12*, and *Ifih1* significantly increased the signal after poly(I:C) stimulation (Figure 5B). To determine how these genes regulate IFN-I signaling, we co-transfected 293T cells with a specific gene plus the genes encoding TRIF in the TLR3/4 pathway (Figure 5C), MAVS in the RIG-I/MDA5 pathway (Figure 5D), STING in the cGAS pathway (Gao et al., 2013; Sun et al., 2013) (Figure 5E), and TBK1 that mediates all three pathways (Figure 5F). In addition to confirming the functions of the three known negative regulators and the positive control of *Ifih1*, our results also showed significant suppression of IFN-β-luciferase activities by eight genes when stimulated with TRIF, by six genes when stimulated with MAVS, and by four genes when stimulated with STING (Figures 5C–5E; Table S10). Furthermore, 10 of the 13 genes (*Ak3*, *Fosl1*, *Inpp4a*, *Havcr2*, *Fcγr1*, *Satb1*, *Selenbp2*, *Helb*, *Helz2*, and *Lrp12*, except *Bc016423*) tested for dose responses showed consistent dose effects in at least one of the co-transfection or stimulation experiments (Figure 6; Table S10),

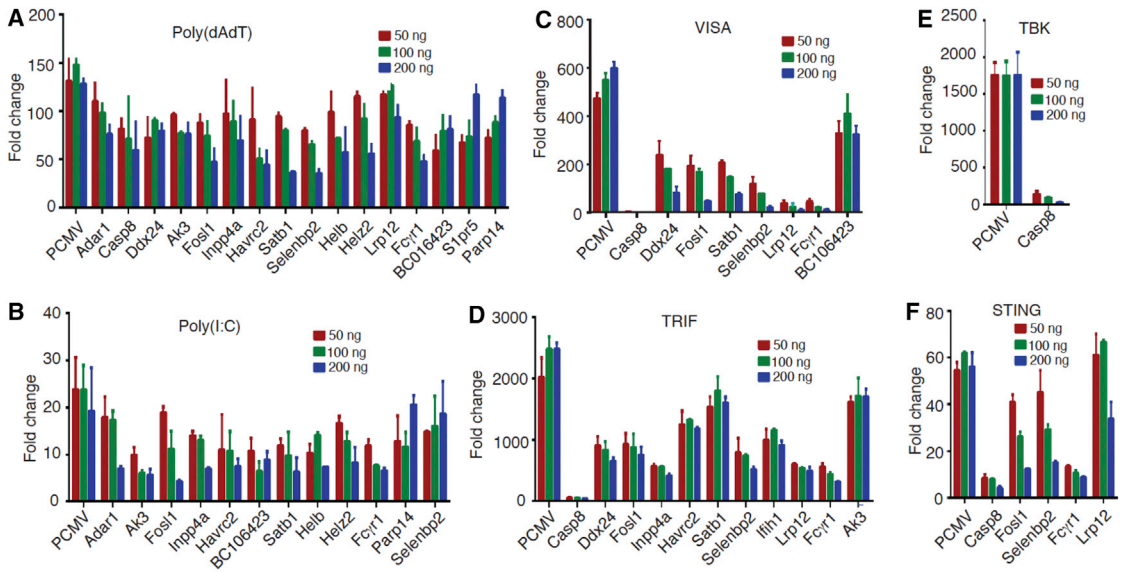

Figure 6. Dose Responses of Luciferase Activities from 293T Cells Transfected with Candidate Genes and Then Stimulated with Poly(dAdT) or Poly(I:C) or Co-transfected with Key Genes in IFN-I Signaling Pathways

(A and B) Transfection of plasmids with genes at indicated dosages and then stimulated with poly(dAdT) (A) or poly(I:C) (B) 24 hr later.

(C–F) Plasmids containing candidate genes were co-transfected with MAVS (C), TRIF (D), TBK (E), or STING (F). Dosages and gene names are as indicated, and SDs were from three replicates.

confirming the relationships of gene expression and changes in IFN-I activation.

shRNA Knockdown and Increased IFN-I Levels

We also used small hairpin RNA (shRNA) to knock down some of the genes, stimulated the cells with poly(I:C) 24 hr after shRNA treatment, and then measured ISRE-luciferase activity 24 hr after stimulation. shRNA knockdown (KD) efficiencies were first determined on western blot using antibodies against the hemagglutinin (HA) tag fused to the 3′ end of the genes. Except for *Fosl1*, *Parp14*, and *Selenbp2* that had moderate reduction in protein levels, the shRNA KDs of gene expression were highly efficient for the rest of the genes (Figure 7A). Compared with those of reference shRNA controls, ISRE-luciferase activities from cells treated with shRNA targeting *Fosl1*, *Fcγr1*, *Gdpd2*, *Havcr2*, *Helb*, *Parp14*, *S1pr5*, *Ak3*, and *Selenbp2*, as well as *Adar1*, *Casp8*, *Ddx24*, *and Nlp12*, were significantly increased (Figure 7A). These results are consistent with those of gene overexpression and further confirm the functions of these genes in suppressing IFN-I response.

Effects of Gene Overexpression on Virus Replication

We next investigated whether the genes could affect vesicular stomatitis virus (VSV) replication, which is highly sensitive to IFN-I, after expression of the candidate genes. We first transfected the 293T cells with the pCMV14 plasmids containing candidate genes and then infected the cells with VSV expressing GFP (VSV-GFP). We counted cells expressing GFP 24 hr after infection using flow cytometry. Significantly more 293T cells transfected with *Ddx24*, *Ak3*, *Satb1*, *and Helb* were infected with the virus compared with vector control, whereas cells transfected with *Mavs* (positive control) had significantly fewer infected cells, as expected (Figure 7B). We also treated transfected cells with IFN-α (5×10^3 U/ml) for 30 min before infection with VSV-GFP. In addition to *Ifih1*, cells transfected with *Casp8*, *Ddx24*, *S1pr5*, *Fcγr1*, and *Lrp12* became more resistant to VSV infection, whereas those transfected with *Adar1* and *Helz2* were more sensitive compared with vector control (Figure 7C). Interestingly, 293T cells transfected with plasmids containing *Casp8*, *S1pr5*, or *Lrp12* also had significantly higher luciferase signals after poly(I:C) stimulation (Figure 5B), suggesting that these genes likely play a role in controlling VSV replication. They also can regulate IFN-I production with different conditions because they act as negative regulators when stimulated with poly(dAdT).

As an additional confirmation of these results, we performed parallel experiments using another set of 16 human genes cloned into the pcDNA3.1 expression vector (again including *Adar1*, *Casp8*, *and Ddx24* as controls). We co-transfected each gene with the genes encoding MDA5 (Figure S3A), RIG-I (Figure S3B), MAVS (Figure S3C), TBK1 (Figure S3D), IKK1 (Figure S3E), and IRF3 (Figure S3F) into 293T cells and measured luciferase expression under the control of the ISRE promoter (ISRE-luciferase). Again, *Adar1*, *Ddx24*, *Fcγr1*, *Ak3*, *Gdpd2*, *Fosl1*, *Havcr2*, *S1pr5*, *Parp14*, *Selenbp2*, *Helb*, and *Nlrp12* significantly ($p < 0.05$) suppressed ISRE-luciferase signals stimulated by one or more proteins in the MDA5/RIG-I/MAVS pathway, although there were some differences with the results obtained using genes expressed in the pCMV14 vector (*Inpp4a*, *Satb1*, *Lrp12*, and *Gdpd2*, and co-transfection with TBK1) (Table S10). The variations in these results could be due to differences in gene sequences (some mouse genes), plasmid vectors and promoters used (IFN-β promoter and pCMV14 versus ISRE promoter and pcDNA3.1), co-transfected genes, or slightly different experimental conditions used in the two laboratories.

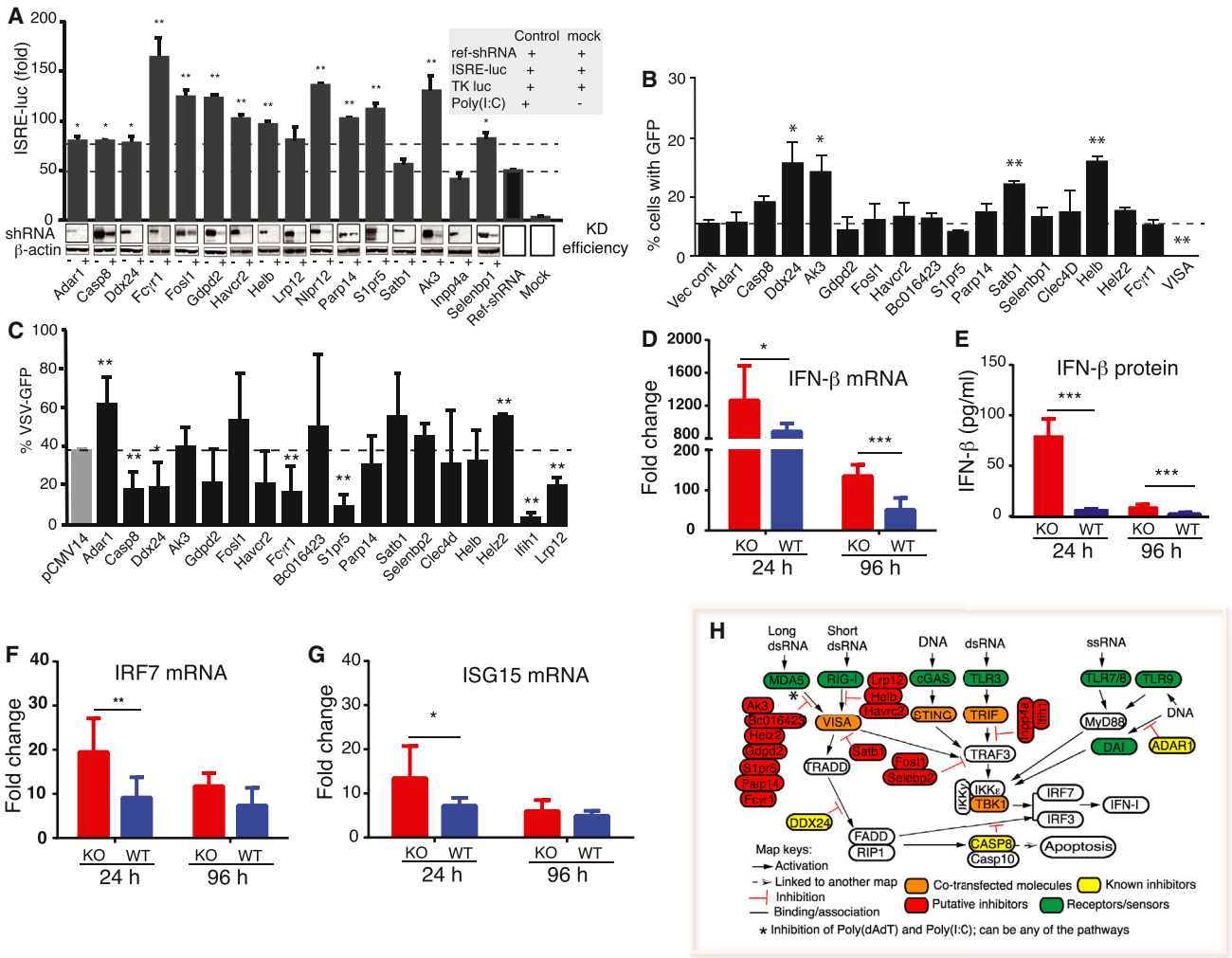

Figure 7. Effects of shRNA Knockdown, Vesicular Stomatitis Virus Infection, or Gene Knockout on IFN-I Response

(A) shRNA knockdown (KD) of various human gene expression in 293T cells significantly increased luciferase signals controlled by interferon-sensitive response element (ISRE) promoter. The KD efficiencies were determined on western blots using antibodies against an HA tag fused to the proteins. β-Actin was used as loading control. The top dashed line indicates significant increase in luciferase signals compared with those of reference shRNA (ref-shRNA) control (bottom dashed line).

(B) Percentage of 293T cells infected with VSV 24 hr after transfection with the pCMV14 plasmid containing the indicated genes. SDs were calculated from three replicates.

(C) Percentage of VSV-GFP-infected cells after treatment with IFN-α and infection with VSV-GFP. The horizontal lines in (B) and (C) are VSV infectivity with vector control.

(D and E) mRNA and protein levels, respectively, of IFN-β in *Fcγr1* KO and WT mice 24 hr and 96 hr postinfection with N67 parasite.

(F and G) mRNA levels of *Irf7* and *Isg15*, respectively, after N67 infection.

(H) Diagram of simplified IFN-I signaling pathways showing putative targeting sites of the negative regulators identified in this study (genes in red background).

For (A)–(G), *p < 0.05; **p < 0.01; ***p < 0.001, t test; SDs from three to four (C) independent replicates.

Nonetheless, there were eight genes (*Ak3*, *Fcγr1*, *Fosl1*, *Havcr2*, *Sipr5*, *Parp14*, *Selenbp2*, *and Helb*) that showed effects on IFN-I activation in both expression vectors performed in two separate laboratories (Table S10).

FCγR1 as a Negative Regulator of IFN-β Response during Parasite Infection

To confirm that FCγR1 functions as a regulator of IFN-I response during parasite infection, we infected *Fcγr1* knockout (KO) mice (Ioan-Facsinay et al., 2002) with N67 parasites and indeed found significantly higher mRNA and protein levels of IFN-β in the *Fcγr1* KO mice than in wild-type (WT) C57BL/6 mice 24 hr and 96 hr p.i. (Figures 7D and 7E). Additionally, the mRNA levels of *Irf7* and *Isg15* were also significantly higher in the KO mice 24 hr p.i. (Figures 7F and 7G). These results demonstrate that FCγR1 can suppress the early IFN-I response during parasite infection and further support the functional prediction derived from GPLS.

DISCUSSION

This genome-wide study shows that interactions between the host and malaria parasite are complex, involving large numbers of both host and parasite genes. Taking advantage of genetic recombination between two parasite strains and progeny that inherited unique combinations of gene sets from each of their parents, we show that the expression of many host genes responding to malaria infection is inheritable and that GPLSs from the host-parasite interaction could provide a basis for functionally clustering host genes. The approach used to cluster host genes is different from the traditional QTL or eQTL. In addition to the large-scale linkages of host genes to parasite genetic loci using QTL analysis, we introduced two concepts in this approach: (1) we mapped ts-eQTLs using phenotypes from the host and genotypes from the parasite; and (2) we used GPLS, in addition to individual LOD scores, to identify host genes in related pathways. The use of GPLSs allows detection of interactions that may have been missed due to individual LOD scores slightly lower than 3.0. By virtue of incorporating a quantitative measure of the genetic variation of the parasite, the GPLS approach could possibly improve the accuracy of gene function predictions, compared with clustering based simply on gene expression levels. There were 24 data points, one from each progeny, for each host gene if we clustered them using expression level directly. In the GPLS, the expression level of each gene was first analyzed for interaction with hundreds of MS markers to derive a second-level data point (LOD scores). The integration of parasite genetic variation into host gene expression transformed simple gene expression levels into measures of host-parasite interaction. The GPLS approach gains bioinformatic power from the combination of large numbers of host gene responses and parasite genetic variation, which were exploited to provide a sensitive method for predicting host gene function. If we clustered genes by expression level alone, we would not have been able to link host genes to parasite loci either. In our hands, the lack of clear clustering pattern and the grouping of the majority of the progeny in clusters separated from the parents suggest that new expressional phenotypes were generated in the progeny and that clustering of gene expression level may not be a good method for functional prediction (Figure S1A). Indeed, we tried various gene expressional clustering, but the results were not satisfactory or comparable to those we had from GPLS. For direct comparison of the GPLS and expression-level clustering, we also grouped 4,603 host genes into 460 clusters (~10 genes per cluster to match the average gene numbers in the GPLS clusters) based on gene expression levels using the same SOM methods. These results show that the genes were clustered quite differently. First, different sets of genes were filtered out due to low differential expression (SD < 0.1) among the progeny. Second, genes in a GPLS cluster generally distributed in multiple expression clusters with different GO terms and vice versa, suggesting different clustering mechanisms. For example, the GPLS clusters 219, 220, and 243 containing 32 mostly known IFN-I-related genes were distributed in 21 different clusters based on gene expression levels (data not shown). We also performed GO-term enrichment on the expressional clusters and obtained FDR values for each cluster (data not shown), although it was difficult to judge which clustering method was better because different GO terms and gene sets were obtained. We next searched for the clusters with "interferon" in both GPLS and expressional clusters containing at least one IFN-I term and found eight GPLS clusters with 83 genes and eight expressional clusters with 85 genes, respectively (Table S11). Again, there were only ten genes shared between the two gene sets. GO-term enrichments of these gene sets showed better FDR values (<0.05) for five out of seven IFN-I-related GO terms using GPLS than when using expression clustering. These analyses confirm that the two approaches produce different clusters and gene sets, and the GPLS is better than expressional clustering in grouping genes with related functions, at least for the IFN-I-induced genes. It should be noted that many genes may have been assigned incorrect or missing some GO terms (functions unknown), and FDR values from enriched GO terms may not correctly reflect the real functions of the genes. The final confirmation of the power of GPLS in predicting gene function came from our experimental verification of the 14 candidate genes (out of 15). The only gene that did not show significant changes after transfection of plasmids was *Clec4d*, which encodes a C-type lectin. Because our functional verification focused on DNA/RNA recognition pathways, experiments testing C-type lectin signaling pathways recognizing carbohydrates may be necessary in order to elucidate the functional role of *Clec4d* in IFN-I response. These analyses, particularly the experimental verification of gene function, demonstrated the high accuracy and validity of the GPLS clustering in predicting genes involved in host-parasite interaction, although we recognized that some of the IFN-I-related genes could also be detected through clustering gene expression levels. We would also like to point out that the phenotypes of host gene expression we measured included signals from changes in gene expression and/or in cell populations of the spleen. Nonetheless, the changes in mRNA levels, either due to alterations in gene expression level or cell populations, represented host responses to parasite infections or the phenotypes we measured.

Another significant contribution of this study is the discovery of many unknown IFN-I regulators. We experimentally verified 14 genes functioning in the regulation of IFN-I responses using various methods. Although most of the experiments were done in vitro, the involvement of these genes in parasite infection or in vivo were implicated because they were clustered together initially based on the gene responses to parasite infections. To further confirm candidate gene function in vivo, we also infected mice with one of the disrupted candidate genes (*Fcgγr1*) and showed that mice without *Fcgγr1* produced significantly higher levels of IFN-β, *Irf7*, and *Isg15* compared with those of WT mice. The demonstration of the *Fcgγr1*gene in regulating IFN-I responses adds another important function in innate response to this receptor that is mainly known for binding immunoglobulin G in adaptive immunity (Ioan-Facsinay et al., 2002). Due to the large number of genes involved, we were not able to dissect the molecular interactions or their precise roles in signaling pathways in this study. Based on our preliminary data, we can only speculate on the potential targeting molecules in the known IFN-I signaling pathways for these IFN-I regulators (Figure 7H); additional functional characterizations

are necessary to fully understand the specific roles of these genes in IFN-I responses.

The identification of negative regulators, instead of pattern-recognition receptors, is likely due to the relatively late sampling time. We sampled mRNA day-4 p.i. because we were initially interested in mechanisms of parasitemia control. The level of IFN-β and many interferon-induced genes peaked on day 2 and returned to low levels after day 4 p.i.(Wu et al., 2014), which is consistent with the activation and identification of negative regulators, not receptors (RIG-I, MDA5) or adaptors such as MAVS or STING that was shown to play an important role in malaria infection (Sharma et al., 2011; Wu et al., 2014). Use of RNA samples from early infection may identify novel receptors and adaptors in pattern recognition and signaling. Although the large datasets involving large numbers of host genes and parasite genetic loci prevent detailed experimental follow-up on each candidate host gene or a parasite locus in this report, our study provides a valuable resource for studying both host and parasite genes, which will greatly enhance our understanding of gene function and host responses to infections and provide new avenues for studying malaria infection in humans.

EXPERIMENTAL PROCEDURES

Parasites and Mice Used in This Study, RNA Preparation, and Microarray Analysis

The procedures for these experiments can be found in Supplemental Experimental Procedures. All the experiments were performed in accordance with NIH-approved animal study protocol LMVR-11E.

Clustering Genes with Similar Genome-wide Pattern of LOD Scores

The linkage of host gene and parasite marker was determined using ANOVA, and the LOD score was calculated as the $\log_{10}$ likelihood ratio using methods described previously (Yuan et al., 2011). Specifically, for each gene-marker pair, progenies were grouped based on their genotype. ANOVA tests were performed to evaluate if there was a significant difference between the expression levels of the different genotype groups, and an LOD ($\log_{10}$ [p value]) was calculated. GPLS plots for specific gene clusters were obtained by plotting the LOD scores in Tables S3 and S5 using the "chart" function in Excel. Clustering of GPLSs was performed using the SOM algorithm (Kohonen, 2006). Only the host genes with an LOD score $\geq$ 2 were used in clustering analysis. The SOM algorithm clustered the LOD score profiles (or expression levels) of genes based on the similarity between the GPLSs measured by pairwise Euclidean distance, and the analysis was performed using the SOM Toolbox (http://www.cis.hut.fi/projects/somtoolbox/), where detailed documentation of the algorithm can be found. Briefly, the SOM was trained and optimized through 14 phases with 38,000 steps in each phase to minimize the distances between the central data vectors and the LOD profiles to form the clusters. The initial learning rate alpha was set to 0.05, which decreased linearly to zero during training. The initial radius of the training area was set to 20 and decreased linearly to one during training. GO term enrichment within each gene cluster or genes significantly linked to a parasite marker was determined using Fisher's exact test, and the p values were corrected for multiple comparisons by controlling the FDR (Benjamini and Yekutieli, 2001). A network of gene-marker interactions was constructed using Cytoscape V3.0 (Shannon et al., 2003). A link was added between every gene-marker pair with an LOD score $\geq$ 3.0.

Transformation of Cell Lines, shRNA KD, and VSV Infection

The detailed procedures for these experiments are described in Supplemental Experimental Procedures. Data from three to four independent experiments were averaged, and the Student's t test was used to estimate the mean differences.

ACCESSION NUMBERS

The microarray data reported in this paper have been deposited in NCBI's Gene Expression Omnibus (http://www.ncbi.nlm.nih.gov/geo/query/acc.cgi?acc=GSE63611) with the accession number GWO: GSE63611.

SUPPLEMENTAL INFORMATION

Supplemental Information includes Supplemental Experimental Procedures, three figures, and 11 tables and can be found with this article online at http://dx.doi.org/10.1016/j.celrep.2015.06.058.

AUTHOR CONTRIBUTIONS

J.W., B.C., W.S., M.L., X.L., S.P., S.M., Y.Q., and S.C.N. performed experiments; R.H. performed data analysis and wrote the manuscript; T.G.M. performed microarray and data analysis and wrote the manuscript; S.B., C.P.A., J.I.C., C.A.L., R.-F.W., and X.-z.S. supervised the experiments, performed data analysis, and wrote the manuscript; and X.-z.S. conceived the project.

ACKNOWLEDGMENTS

This work was supported by the Division of Intramural Research at the National Institute of Allergy and Infectious Diseases (NIAID) and the National Center for Advancing Translational Sciences (NCATS), National Institutes of Health (NIH), by Project 111 of the State Bureau of Foreign Experts and Ministry of Education of China (B06016), and supported in part by grants from the National Cancer Institute, NIH (R01CA090327 and R01CA101795) to R.-F.W. B.C. and M.L. were supported in part by the Chinese Scholar Council. We thank Dr. J.S. Verbeek for the *Fcgr1* KO mice and Cindy Clark of the NIH Library for editing.

Received: December 16, 2014
Revised: March 2, 2015
Accepted: June 16, 2015
Published: July 16, 2015

REFERENCES

Barber, G.N. (2011). Innate immune DNA sensing pathways: STING, AIMII and the regulation of interferon production and inflammatory responses. Curr. Opin. Immunol. *23*, 10–20.

Barreiro, L.B., Tailleux, L., Pai, A.A., Gicquel, B., Marioni, J.C., and Gilad, Y. (2012). Deciphering the genetic architecture of variation in the immune response to Mycobacterium tuberculosis infection. Proc. Natl. Acad. Sci. USA *109*, 1204–1209.

Benjamini, Y., and Yekutieli, D. (2001). The control of the false discovery rate in multiple testing under dependency. Ann. Stat. *29*, 1165–1188.

Boivin, G.A., Pothlichet, J., Skamene, E., Brown, E.G., Loredo-Osti, J.C., Sladek, R., and Vidal, S.M. (2012). Mapping of clinical and expression quantitative trait loci in a sex-dependent effect of host susceptibility to mouse-adapted influenza H3N2/HK/1/68. J. Immunol. *188*, 3949–3960.

Bottomly, D., Ferris, M.T., Aicher, L.D., Rosenzweig, E., Whitmore, A., Aylor, D.L., Haagmans, B.L., Gralinski, L.E., Bradel-Tretheway, B.G., Bryan, J.T., et al. (2012). Expression quantitative trait Loci for extreme host response to influenza a in pre-collaborative cross mice. G3 (Bethesda) *2*, 213–221.

Büngener, W. (1979). [Malaria plasmodia in the mouse. Parasitization of mature and immature erythrocytes by Plasmodium berghei, Plasmodium yoelii and Plasmodium chabaudi (author's transl)]. Tropenmed. Parasitol. *30*, 198–205.

Carlton, J.M., Angiuoli, S.V., Suh, B.B., Kooij, T.W., Pertea, M., Silva, J.C., Ermolaeva, M.D., Allen, J.E., Selengut, J.D., Koo, H.L., et al. (2002). Genome sequence and comparative analysis of the model rodent malaria parasite Plasmodium yoelii yoelii. Nature *419*, 512–519.

Chapman, M.S., Wu, L., Amatucci, A., Ho, S.N., and Michaelson, J.S. (2013). TWEAK signals through JAK-STAT to induce tumor cell apoptosis. Cytokine *61*, 210–217.

Degner, J.F., Pai, A.A., Pique-Regi, R., Veyrieras, J.B., Gaffney, D.J., Pickrell, J.K., De Leon, S., Michelini, K., Lewellen, N., Crawford, G.E., et al. (2012). DNase I sensitivity QTLs are a major determinant of human expression variation. Nature *482*, 390–394.

Eskan, M.A., Rose, B.G., Benakanakere, M.R., Lee, M.J., and Kinane, D.F. (2008). Sphingosine 1-phosphate 1 and TLR4 mediate IFN-beta expression in human gingival epithelial cells. J. Immunol. *180*, 1818–1825.

Fairfax, B.P., Humburg, P., Makino, S., Naranbhai, V., Wong, D., Lau, E., Jostins, L., Plant, K., Andrews, R., McGee, C., and Knight, J.C. (2014). Innate immune activity conditions the effect of regulatory variants upon monocyte gene expression. Science *343*, 1246949.

Gao, D., Wu, J., Wu, Y.T., Du, F., Aroh, C., Yan, N., Sun, L., and Chen, Z.J. (2013). Cyclic GMP-AMP synthase is an innate immune sensor of HIV and other retroviruses. Science *341*, 903–906.

Gazzinelli, R.T., Kalantari, P., Fitzgerald, K.A., and Golenbock, D.T. (2014). Innate sensing of malaria parasites. Nat. Rev. Immunol. *14*, 744–757.

George, C.X., Gan, Z., Liu, Y., and Samuel, C.E. (2011). Adenosine deaminases acting on RNA, RNA editing, and interferon action. J. Interferon Cytokine Res. *31*, 99–117.

Ioan-Facsinay, A., de Kimpe, S.J., Hellwig, S.M., van Lent, P.L., Hofhuis, F.M., van Ojik, H.H., Sedlik, C., da Silveira, S.A., Gerber, J., de Jong, Y.F., et al. (2002). FcgammaRI (CD64) contributes substantially to severity of arthritis, hypersensitivity responses, and protection from bacterial infection. Immunity *16*, 391–402.

Kohonen, T. (2006). Self-organizing neural projections. Neural Netw. *19*, 723–733.

Larsson, J., and Karlsson, S. (2005). The role of Smad signaling in hematopoiesis. Oncogene *24*, 5676–5692.

Lee, M.N., Ye, C., Villani, A.C., Raj, T., Li, W., Eisenhaure, T.M., Imboywa, S.H., Chipendo, P.I., Ran, F.A., Slowikowski, K., et al. (2014). Common genetic variants modulate pathogen-sensing responses in human dendritic cells. Science *343*, 1246980.

Li, J., Pattaradilokrat, S., Zhu, F., Jiang, H., Liu, S., Hong, L., Fu, Y., Koo, L., Xu, W., Pan, W., et al. (2011). Linkage maps from multiple genetic crosses and loci linked to growth-related virulent phenotype in Plasmodium yoelii. Proc. Natl. Acad. Sci. USA *108*, E374–E382.

Li, L., Zhang, X., and Zhao, H. (2012). eQTL. Methods Mol. Biol. *871*, 265–279.

Liehl, P., and Mota, M.M. (2012). Innate recognition of malarial parasites by mammalian hosts. Int. J. Parasitol. *42*, 557–566.

Liehl, P., Zuzarte-Luís, V., Chan, J., Zillinger, T., Baptista, F., Carapau, D., Konert, M., Hanson, K.K., Carret, C., Lassnig, C., et al. (2014). Host-cell sensors for Plasmodium activate innate immunity against liver-stage infection. Nat. Med. *20*, 47–53.

Linkermann, A., Stockwell, B.R., Krautwald, S., and Anders, H.J. (2014). Regulated cell death and inflammation: an auto-amplification loop causes organ failure. Nat. Rev. Immunol. *14*, 759–767.

Ma, Z., Moore, R., Xu, X., and Barber, G.N. (2013). DDX24 negatively regulates cytosolic RNA-mediated innate immune signaling. PLoS Pathog. *9*, e1003721.

Miller, J.L., Sack, B.K., Baldwin, M., Vaughan, A.M., and Kappe, S.H. (2014). Interferon-mediated innate immune responses against malaria parasite liver stages. Cell Rep. *7*, 436–447.

Mogensen, T.H. (2009). Pathogen recognition and inflammatory signaling in innate immune defenses. Clin. Microbiol. Rev. *22*, 240–273.

Nair, S.C., Pattaradilokrat, S., Zilversmit, M.M., Dommer, J., Nagarajan, V., Stephens, M.T., Xiao, W., Tan, J.C., and Su, X.Z. (2014). Genome-wide polymorphisms and development of a microarray platform to detect genetic variations in Plasmodium yoelii. Mol. Biochem. Parasitol. *194*, 9–15.

Pan, Y., Li, R., Meng, J.L., Mao, H.T., Zhang, Y., and Zhang, J. (2014). Smurf2 negatively modulates RIG-I-dependent antiviral response by targeting VISA/MAVS for ubiquitination and degradation. J. Immunol. *192*, 4758–4764.

Pattaradilokrat, S., Li, J., Wu, J., Qi, Y., Eastman, R.T., Zilversmit, M., Nair, S.C., Huaman, M.C., Quinones, M., Jiang, H., et al. (2014). Plasmodium genetic loci linked to host cytokine and chemokine responses. Genes Immun. *15*, 145–152.

Peng, Y., Xu, R., and Zheng, X. (2014). HSCARG negatively regulates the cellular antiviral RIG-I like receptor signaling pathway by inhibiting TRAF3 ubiquitination via recruiting OTUB1. PLoS Pathog. *10*, e1004041.

Rajput, A., Kovalenko, A., Bogdanov, K., Yang, S.H., Kang, T.B., Kim, J.C., Du, J., and Wallach, D. (2011). RIG-I RNA helicase activation of IRF3 transcription factor is negatively regulated by caspase-8-mediated cleavage of the RIP1 protein. Immunity *34*, 340–351.

Reilly Ayala, H.B., Wacker, M.A., Siwo, G., and Ferdig, M.T. (2010). Quantitative trait loci mapping reveals candidate pathways regulating cell cycle duration in Plasmodium falciparum. BMC Genomics *11*, 577.

Rusinova, I., Forster, S., Yu, S., Kannan, A., Masse, M., Cumming, H., Chapman, R., and Hertzog, P.J. (2013). Interferome v2.0: an updated database of annotated interferon-regulated genes. Nucleic Acids Res. *41*, D1040–D1046.

Sakaguchi, S., Yamaguchi, T., Nomura, T., and Ono, M. (2008). Regulatory T cells and immune tolerance. Cell *133*, 775–787.

Shannon, P., Markiel, A., Ozier, O., Baliga, N.S., Wang, J.T., Ramage, D., Amin, N., Schwikowski, B., and Ideker, T. (2003). Cytoscape: a software environment for integrated models of biomolecular interaction networks. Genome Res. *13*, 2498–2504.

Sharma, S., DeOliveira, R.B., Kalantari, P., Parroche, P., Goutagny, N., Jiang, Z., Chan, J., Bartholomeu, D.C., Lauw, F., Hall, J.P., et al. (2011). Innate immune recognition of an AT-rich stem-loop DNA motif in the Plasmodium falciparum genome. Immunity *35*, 194–207.

Sun, L., Wu, J., Du, F., Chen, X., and Chen, Z.J. (2013). Cyclic GMP-AMP synthase is a cytosolic DNA sensor that activates the type I interferon pathway. Science *339*, 786–791.

van der Harst, P., Zhang, W., Mateo Leach, I., Rendon, A., Verweij, N., Sehmi, J., Paul, D.S., Elling, U., Allayee, H., Li, X., et al. (2012). Seventy-five genetic loci influencing the human red blood cell. Nature *492*, 369–375.

Wang, Z., Choi, M.K., Ban, T., Yanai, H., Negishi, H., Lu, Y., Tamura, T., Takaoka, A., Nishikura, K., and Taniguchi, T. (2008). Regulation of innate immune responses by DAI (DLM-1/ZBP1) and other DNA-sensing molecules. Proc. Natl. Acad. Sci. USA *105*, 5477–5482.

Wu, J., Tian, L., Yu, X., Pattaradilokrat, S., Li, J., Wang, M., Yu, W., Qi, Y., Zeituni, A.E., Nair, S.C., et al. (2014). Strain-specific innate immune signaling pathways determine malaria parasitemia dynamics and host mortality. Proc. Natl. Acad. Sci. USA *111*, E511–E520.

Yuan, J., Cheng, K.C., Johnson, R.L., Huang, R., Pattaradilokrat, S., Liu, A., Guha, R., Fidock, D.A., Inglese, J., Wellems, T.E., et al. (2011). Chemical genomic profiling for antimalarial therapies, response signatures, and molecular targets. Science *333*, 724–729.